

# At-Sea Summary of Microstructure Profiling During EPIC 2001

M.C. Gregg, D.P. Winkel, J. Mickett, G. Carter,  
J. Miller, E. Krause, A. Bartlett, P. Aguilar

October 4, 2001

## Abstract

Operations went smoothly, allowing us to do everything we planned. Because the weather varied from clear skies and flat seas to the spinup of a hurricane, we sampled a wide range of atmospheric forcings. Only twice were operations halted unexpectedly: the bridge ordered the decks cleared when lightening was all around and intense. The first episode lasted almost 5 hours and the second about 2.

Our MMP profilers stabilize below 2-3 m, but the ship's wake dominated the shallow signal, as expected. Propellers on the Z-drives produce deeper turbulence than we experience on ships with conventional propulsion. Using the standard criterion of a  $0.01 \text{ kg m}^{-3}$  density increase, mixed layer depths ranged from a few meters to 29 m. Often the layers were stabilized by salinity. Determining whether any of the dissipation rates from the mixed layer are free of ship contamination will be one of the largest challenges in our analysis. For this summary, we have removed all of them in the figures focusing on shallowing mixing.

Mixing at the base of the mixed layer is the most important issue for air-sea coupling, and we experienced a wide range of states. These data are assumed to be uncontaminated by the ship, but this too will be checked carefully. Figure 4 shows the evolution of temperature, salinity, and density in the surface layer, Figure 15 shows the shallow diapycnal diffusivity and buoyancy flux.

Near-inertial motions dominated the upper 300 m while we were on station, across the base of the mixed layer, in the thermocline, and below. Their intensity increased substantially half way through, in the aftermath of strong winds. To varying degrees, shear,  $N^2$ ,  $\epsilon$ , and  $K_\rho$  carry signatures of the sloping near-inertial phase lines.

As near-inertial energy increased, the sharp thermocline thickened, as did the near-surface zone of elevated dissipation rates. Coincident with this was a deepening wedge of warmer and saltier water. These changes eventually filled the upper 300 m, as did similar changes in dissolved oxygen concentration. Below the thermocline, the diapycnal diffusivities were so low, averaging slightly more than  $10^{-6} \text{ m s}^{-2}$ , that it is

inconceivable that mixing produced the changes. Understanding how these water mass changes were linked to the varying near-inertial energy looks at this point to be the most interesting and puzzling issue to understand.

# 1 Sampling

## 1.1 Modular Microstructure Profiler (MMP)

Two test drops were taken with each profiler en route to station. These were drops 12300–12305. The drops on station were 12306–13485;

During time on station, the ship remained within 5 nm of a circle centered at  $9^{\circ}, 56'N$ ,  $95^{\circ}0'W$ . This was offset from the TAO mooring to avoid interference. The last position of the mooring was  $10^{\circ}01.3'N$ ,  $94^{\circ}53.8'W$ . The Coriolis frequency was  $f = 2.50 \times 10^{-5} \text{ s}^{-1}$ , giving an inertial period of 69.8195 hr or 2.9091 d.

Profiles were taken to 3 MPa at average fall rates of  $0.65 \text{ m s}^{-1}$ . For the last 10 hours the fall rate was slowed to about  $0.35 \text{ m s}^{-1}$  in an attempt to resolve temperature microstructure.

MMP sampling on station started with drop=12306 at 1832 UTC 12 September (yday=254.7787) and ended with drop=13485 at 0432 UTC 1 October (yday=273.1978), for a total of 1180 profiles on station. These yeardays are calculated with midnight on Dec 31 as day 0.0 and are one day less than Julian days. They measure days elapsed since the year began, as used in computing tides.

Figure 1 summarizes the sampling. The top panel shows the intervals in minutes between successive drops. The longest interval, almost 5 hours, occurred during day 258 when lightning around the ship cleared the deck. A similar, but shorter, gap occurred on day 265. The median interval was 15.6 minutes. Taking time out for diving on the buoy, to recover sensors, created a gap nearly the same length during day 270.

Binning the data in 3-hour intervals yielded 1 to 14 profiles per bin (middle panel). The median is 8. Increasing the interval to 4 hours smooths the fluctuations, but does not remove the minima of 1.

Sampling was less during daylight owing to the need to take radiance profiles, do a CTD cast near noon, and have the ship oriented to receive SEAWIFS data.

MMP1 was used the most, for 521 profiles. Because it was twice shut down for repairs, MMP2 was used the least, collecting 299 profiles. The first gap started during yday 255 and ended during 259. The second gap began during yday 264 and lasted into yday 266. MMP3 took 360 profiles.

MMP data are plotted against sea pressure in MPa; 1 MPa equals 100 decibars or a depth of nearly 100 m.

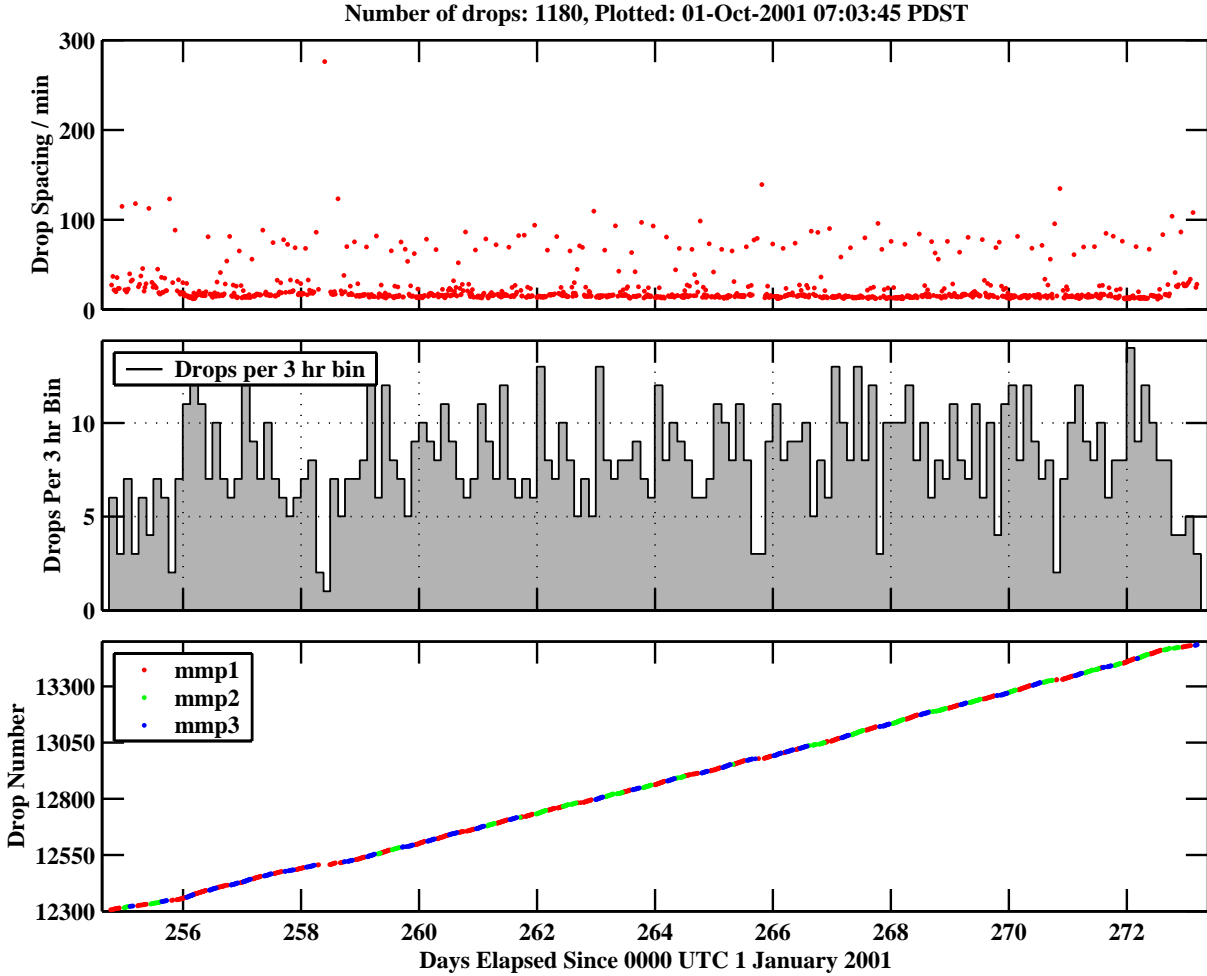


Figure 1: Summary of MMP sampling.

## 1.2 Expendable Current Profilers (XCPs)

XCPs were dropped at approximately 8 hour intervals between 1621 UTC, 19 September (yday=261.6813) to 2323 UTC on 24 September (yday=266.9743). The interval was chosen to sample the approximately 3-day inertial period.

## 2 Cruise-Average Profiles

The average profiles (Fig. 2) show the surface mixed layer with nearly constant temperature and a large salinity gradient, which is easy to understand in view of the heavy rain. We believe that dissolved oxygen was close to saturation near the surface but need to obtain

the function for saturation in terms of temperature. All profiles had a decrease in the first few meters. Is this an instrument artifact?

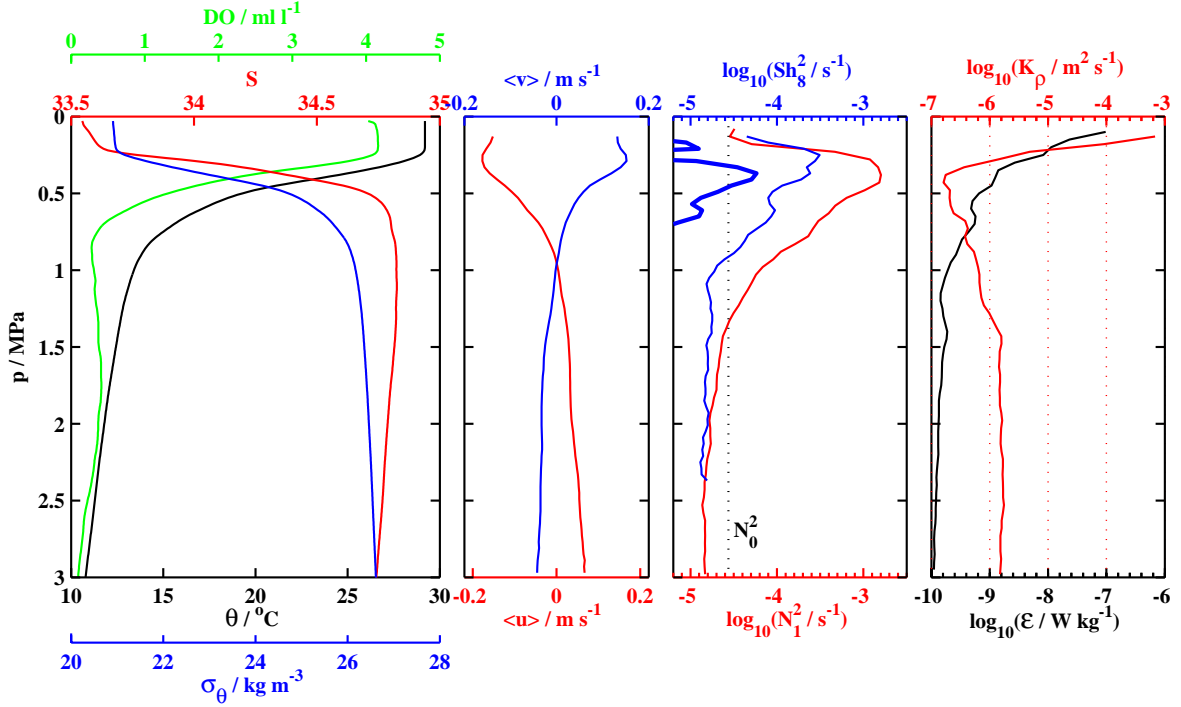


Figure 2: Cruise-average profiles.  $\theta$ ,  $S$ ,  $\sigma_\theta$ , and  $N^2$ , DO, and  $\epsilon$  were gridded at 0.01 MPa intervals before time averaging. In the third panel, the dark blue line is the square of the mean shear, and the light blue line is the sum of that and the square of the shear fluctuations.

The ADCP recorded data as vertical bins of 4 m and 1 minute time averages. Because the ship's velocity from GPS was not available, 8-m-shear was calculated as

$$z = \frac{\sum_{i=1}^{i=4} z_i}{4}, \quad Sh8x(z_i) = \frac{u_i - u_{i-2}}{2\Delta z} + \frac{u_{i-1} - u_{i-3}}{\Delta z} \quad (1)$$

where  $z$  is upward, but ADCP array indices increase downward. Integrating the shears gave the velocity profiles in Figure 2. They are plotted with zero mean values.

Assuming that the velocities are close to zero at 3 MPa, the mean velocity of the surface layer is about  $0.18 \text{ m s}^{-1}$  toward the northwest. We need to compare the velocities with the current meter record on the TAO mooring and to examine their frequency content. The  $u$  and  $v$  components are so symmetric, that the means could be aliased near-inertial motions. These shears are first-differences of velocity over 8 m, taken at 4 m intervals.

The third panel compares the average of  $N^2$  computed over 1 m intervals with the 8-m shears. The dark blue curve is the square of the mean shear, i.e.  $\langle \frac{\Delta u}{\Delta z} \rangle^2 + \langle \langle \frac{\Delta v}{\Delta z} \rangle \rangle^2$ . It is so much less than  $\langle N^2 \rangle$  that mean shear should have played little role in mixing.

The light blue curve is the sum of that and the average fluctuating shear variance, i.e. the total shear variance. It is constant below 1 MPa and rises sharply below 2.4 MPa, where the plot is cut off. It seems likely that the data are noisy below 1 MPa. Otherwise, the shear variance should continue decreasing in concert with falling  $N^2$ . We need to look carefully at the characteristics of the ADCP data.

The dissipation rates were put on a 0.01 MPa grid in the vertical and one column per drop. Many plankton impacts remain in the data, so  $\log_{10}$  was taken of the array and then a second order median filter was applied to the matrix. Since  $\epsilon$  data are nearly lognormal, the median filter is an excellent way to remove outliers, The array was then averaged in 0.05 MPa vertical bins to form the average profile shown.

The average dissipation was reasonably high in the thermocline, but decreased rapidly as  $N^2$  decreased. Below 1 MPa, the average was barely above our noise level of -10.  $K_\rho$  was significant in the thermocline, but near molecular at the peak-N and then rose to slightly above -6. If we set individual estimates of  $\log \epsilon = -10$  to zero, because there are our noise level, the averages would be even smaller.

### 3 Temperature, Salinity, and Density

Mixed layer temperatures warmed during the first half of the cruise and then cooled the remainder while the layer deepened slightly (Fig. 3). This plot is a pcolor of the first profile subtracted from every profile at .01 MPa vertical resolution. The grainy structure has about the time scale of instrument changes and indicates calibration errors between the 3 MMPs.

Temperature changed even more below the mixed layer, beginning just below the layer and extending downward with time.

The surface salinity appeared to increase after the first burst, indicating that the calibration of MMP1 was initially low or something else produced incorrect low values only during the first burst. Ignoring the first burst, mixed layer salinities remained approximately uniform until day 266 when they freshened for several days before increasing again. This was a result of the very heavy rain. Between 0.35 and 1.6 MPa the water freshened while salinity increased from 1.6 to 2.15 MPa. The zone of freshening also was cooler than the initial profile. Gradually this zone contracted vertically about a core centered at 1.5 MPa, finally ending on day 267. At other depths the water became saltier as the water warmed.

Density shows the same pattern of change deepening from the surface, but lacks the structures between 1.3-1.5 MPa during days 258-265. These were thermohaline intrusions that were nearly compensated in density. Except for a slight initial increase in the lower half of the profiles, density steadily decreased compared to the initial profile.

Figure 4 shows a more detail view near the surface, with the mixed layer depth overlaid on each plot.

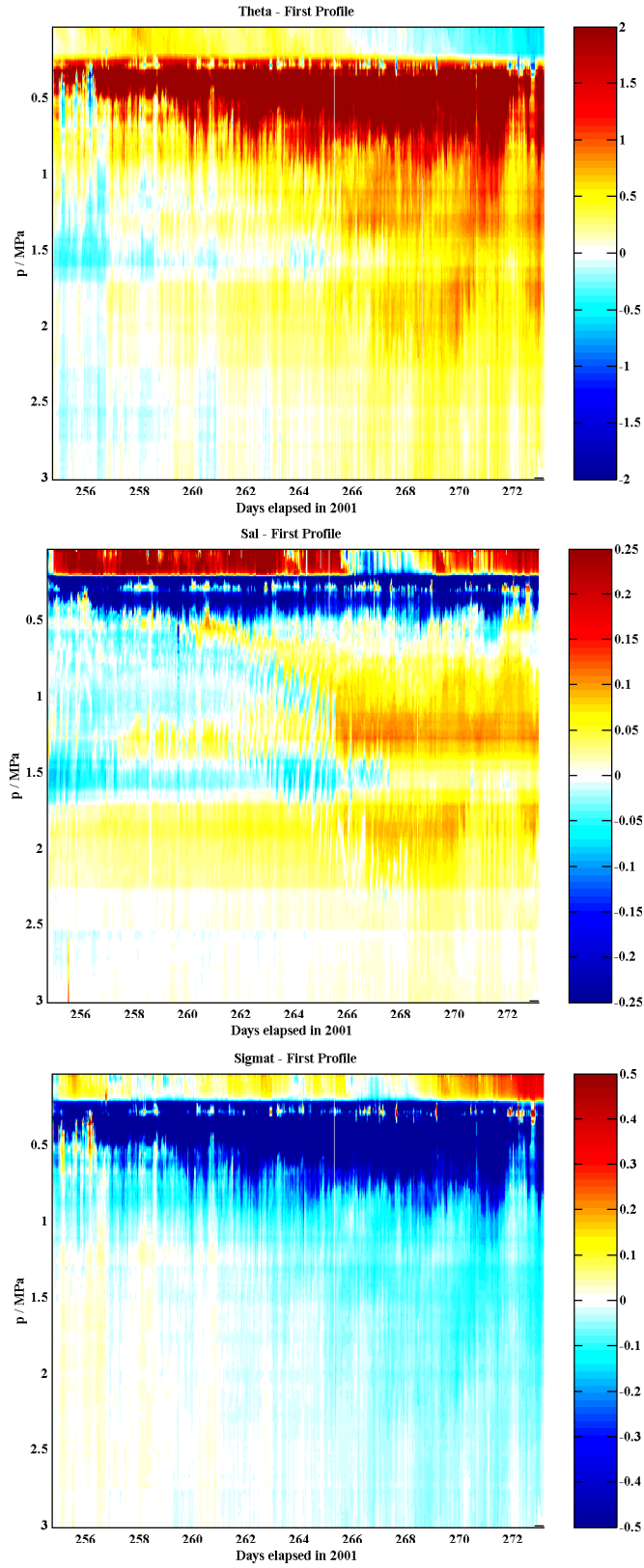


Figure 3: Potential temperature (top), salinity (middle), and potential temperature (bottom) of every profile minus the first profile.

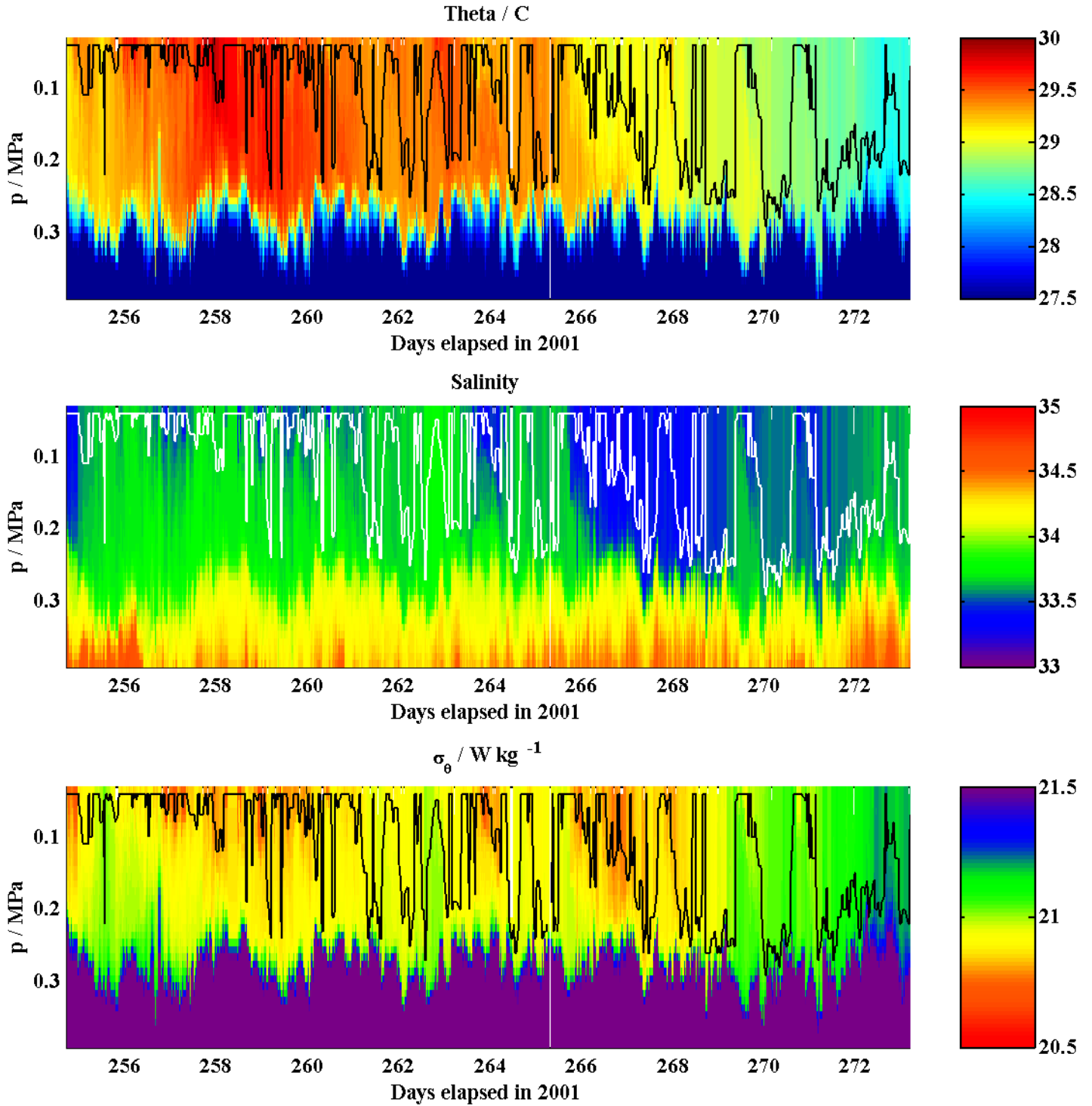


Figure 4: Expanded view near the surface of from top to bottom,  $\theta$ ,  $S$ , and  $\sigma_{\theta}$ . The line overlaid on the plots is the mixed layer depth, calculated as the depth where  $\Delta\sigma_{\theta} = 0.01 \text{ kg m}^{-3}$  greater than the shallowest value measured.



## 4 Dissolved Oxygen

MMP1 and MMP2 carried the new Sea-Bird dissolved oxygen probes. The probes do not fit on MMP3 owing to the acoustic current meter. The sensor seemed to work well and gave interesting data, showing oxygen anomalies that came and went with the thermohaline intrusions below the thermocline. The overall pattern is similar to those of temperature, salinity, and density, particularly the deep positive anomalies.

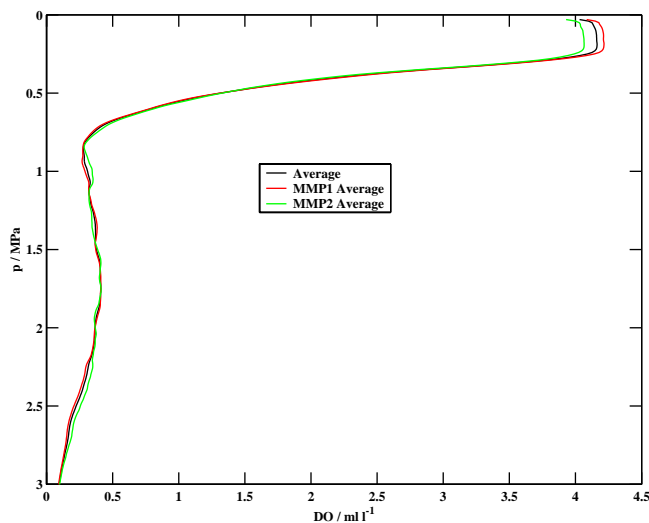


Figure 5: Average DO computed several days before the cruise ended. The black line is an average of all drops with good oxygen. Red and green lines are averages using only MMP1 or MMP2. MMP1 and MMP2 differ about  $0.15 \text{ ml l}^{-1}$  in the mixed layer. The greater number of drops with MMP1 weights the overall average toward it.

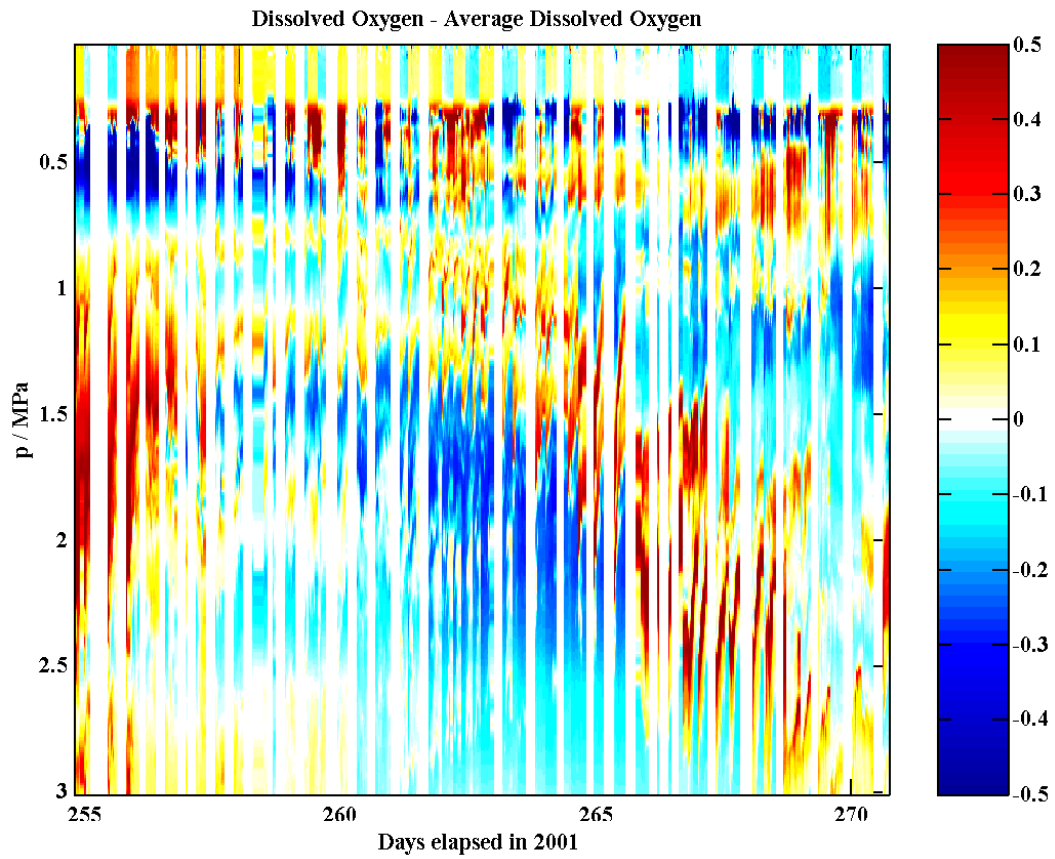


Figure 6: pcolor of Dissolved Oxygen fluctuations, i.e. of DO minus the average profile. White bands are when MMP3 was being used and no DO was measured.

## 5 ADCP Velocity

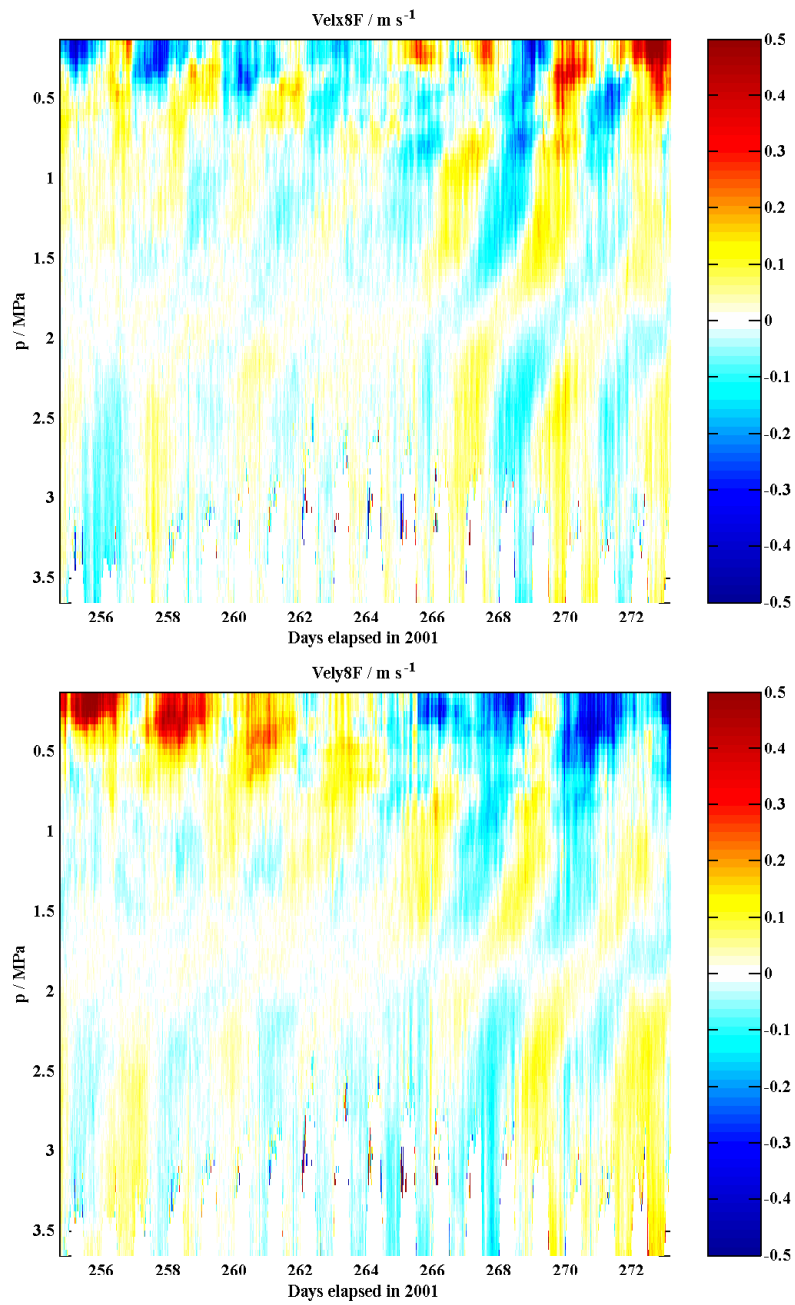


Figure 7: Eastward (upper) and northward (lower) velocities. The data were averaged over 15 minutes and time and referenced to the average velocity between 150 and 220 m.

Velocities are dominated by near-inertial motions, demonstrated by: the  $u$  and  $v$  components being in quadrature, a period of approximately 3 days, and upward-propagating phase lines (Fig. 7). Initially weak, the intensity of the motions increased until yday 269 and remained high until the end.

The odd kinks in the phase lines near 2 MPa result from our referencing the ADCP velocities to that depth range and are an artifact of on-board processing to compensate for the misalignment of the ship's ADCP transducers. The kinks are not present in the shear components (Fig. 8). Note the change in slope of the phase lines in the thermocline.

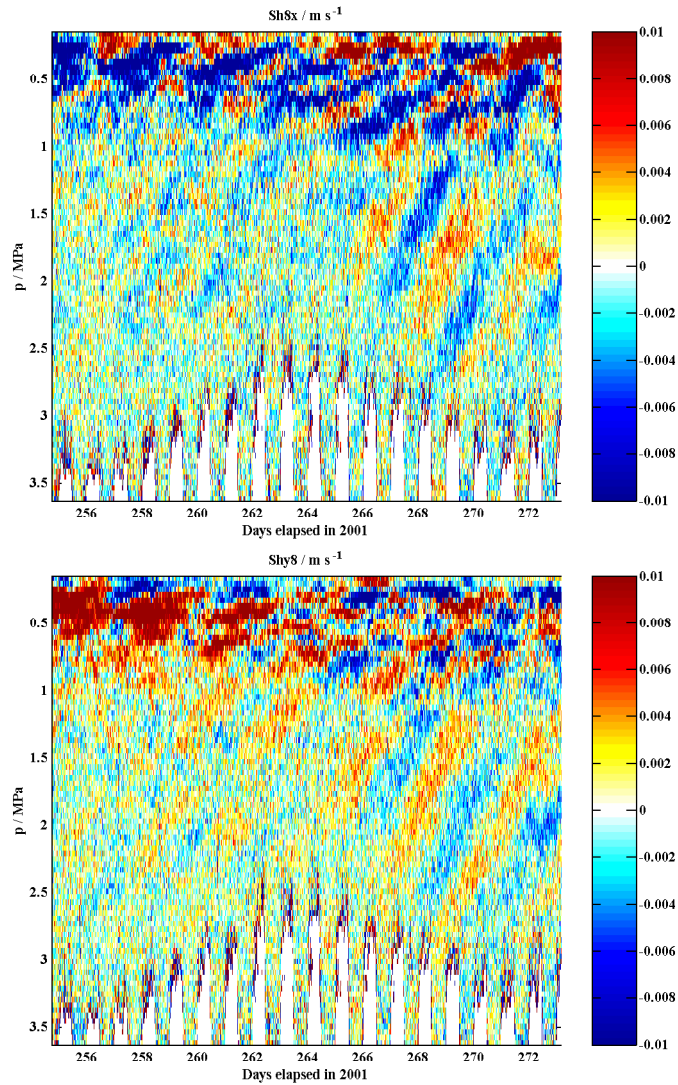


Figure 8: Shear components,  $\Delta u / \Delta z$  above and  $\Delta v / \Delta z$  below.

Shear variance increase in and below the thermocline as the near-inertial motions increased in intensity (Fig. 9). Hints of the upward-sloping phase lines remain, consistent with the motions being near-inertial rather than inertial.

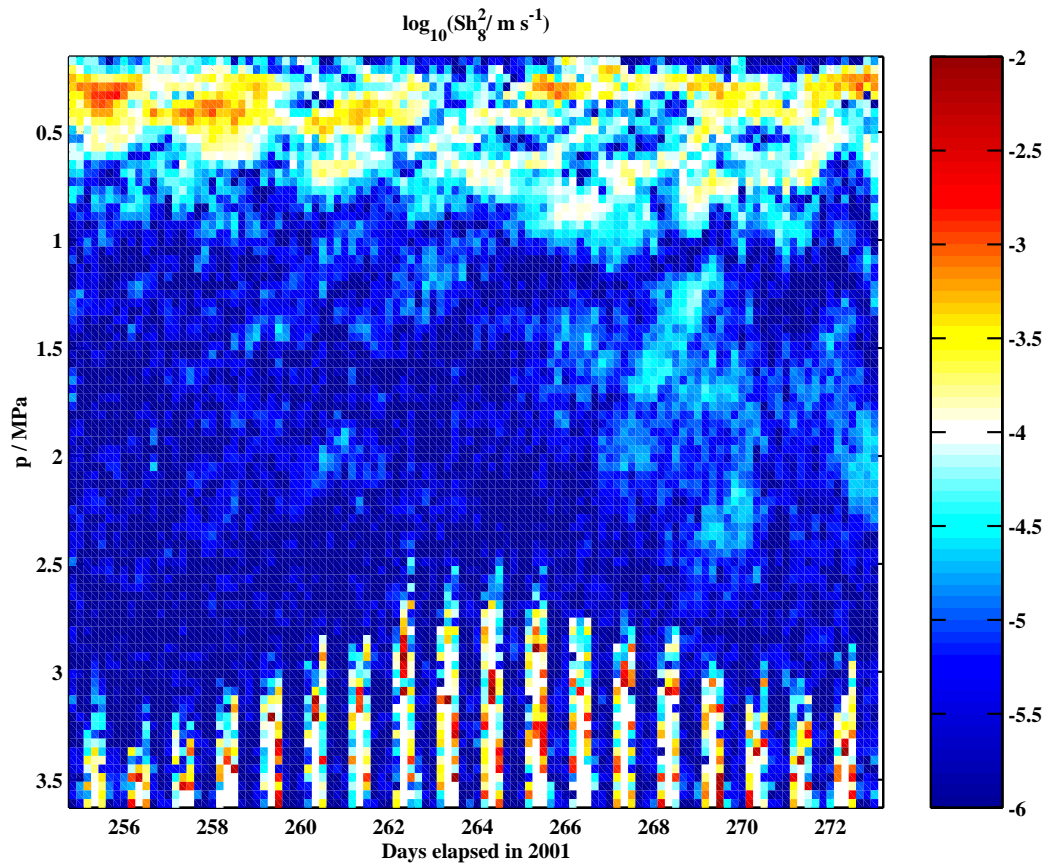


Figure 9: Shear squared averaged over 4 hours and with interpolated shading.

## 6 $N^2$

As shown in Figure 10, the thermocline thickened perhaps by 50% between ydays 255 and 266. It seemed to be thinning a day before we left.

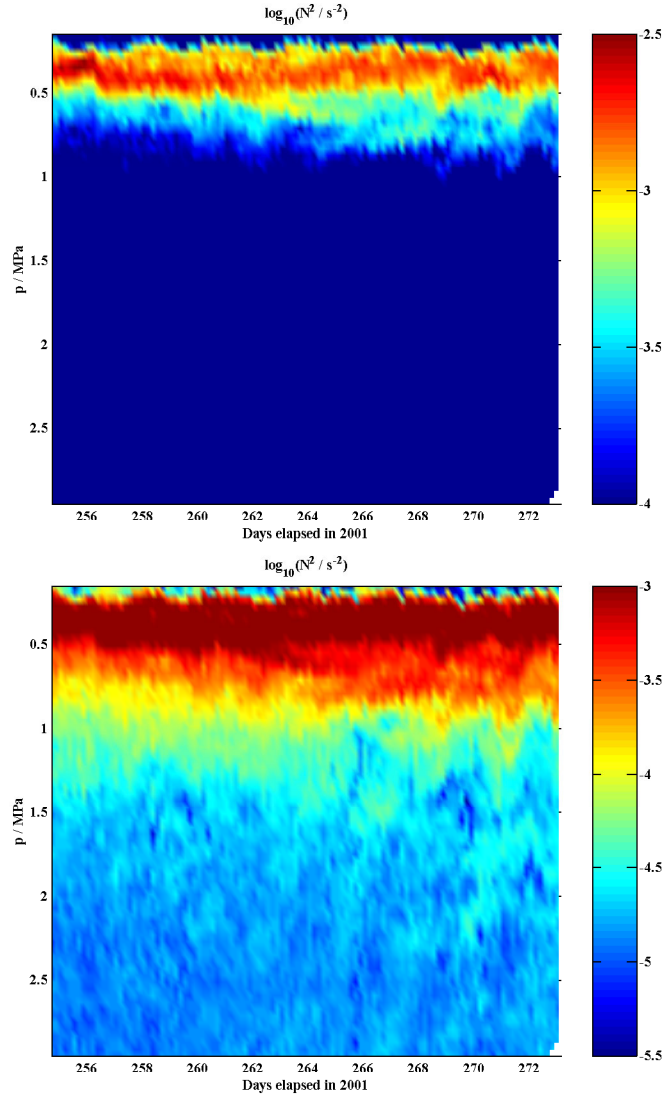


Figure 10:  $\log_{10}N^2$  with  $N^2$  calculated by first differencing over 0.08 MPa intervals every 0.04 MPa and averaging profiles in 4 hour time bins. Top: Color axis chosen to highlight the thermocline. Bottom: Color axis chosen to highlight deeper stratification.

Stratification fluctuated significantly, particularly as the thermocline thickened and, during the second half of the cruise, below the thermocline (Fig. reffig.logNsqFluct). From day

257 to 261 the peak- $N$  remained near 0.5 MPa. From 261 to 266 it deepened to about 0.65 MPa as the thermocline thickened. Beginning during day 264, there are hints of parallel bands where the near-inertial motions were most intense. These can also be seen in the lower panel of Fig 10.

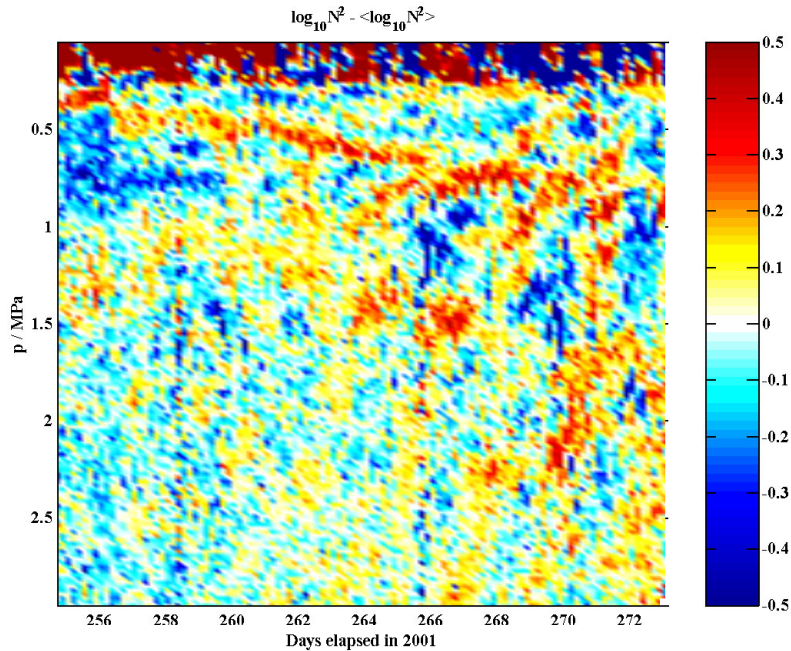


Figure 11:  $\log_{10} N^2$  minus the log of the array average, showing where stratification was stronger and weaker than average. Except for the low stratification near 0.75 MPa from days 255-260, most of the variability was below the thermocline and where the near-inertial motions were most intense.

## 7 Froude Number

The Froude number,  $Fr_8^2 \equiv Sh_8^2 / N_8^2$ , has some of its largest values below the thermocline where the near-inertial waves were most intense. Not visible on printed plots, even early in the cruise, lines of  $\epsilon$  barely above background slope upward with the same slopes as the near-inertial shears. Froude numbers are less than the 4 needed for shear instability because the ADCP does not resolve all of the important shear.

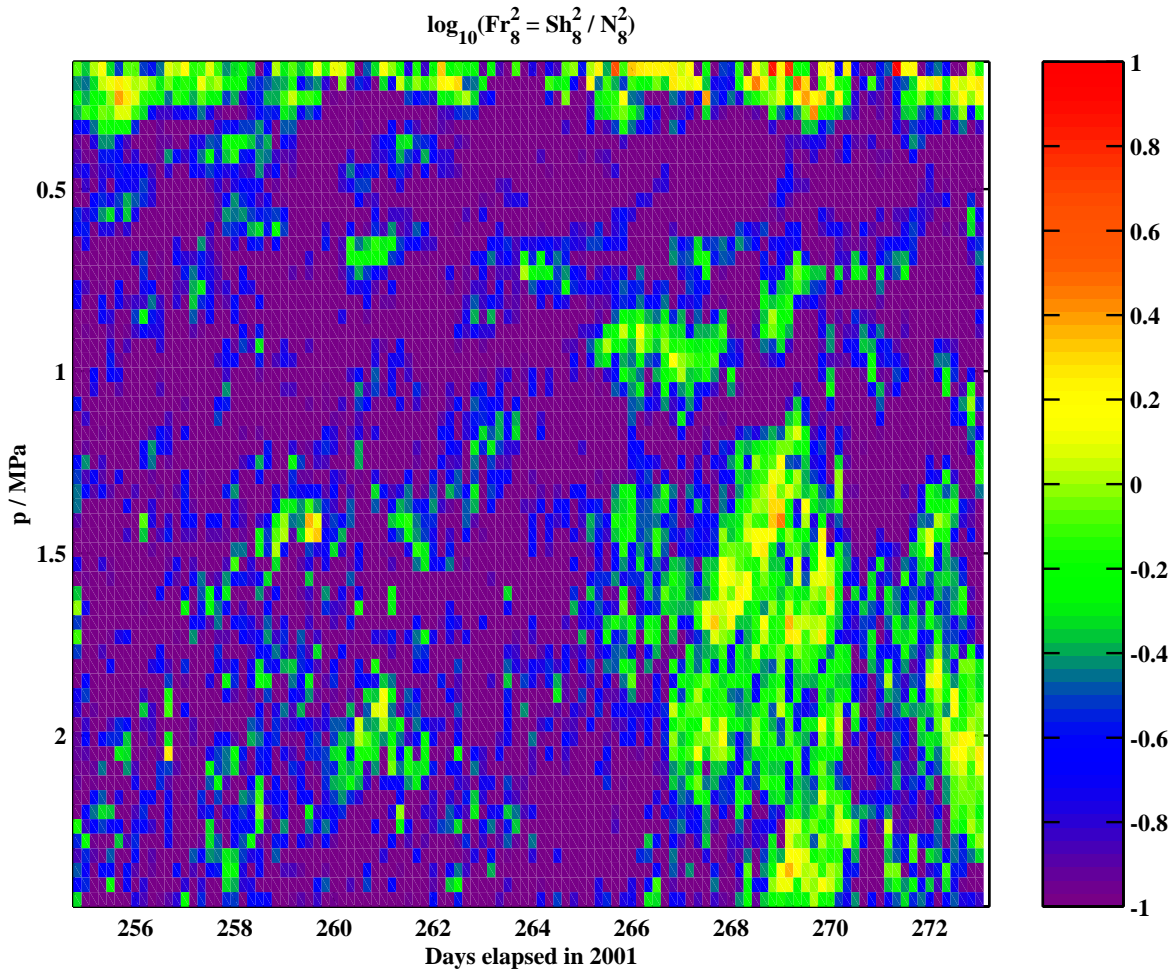


Figure 12: Froude number computed using  $Sh_8^2$  and  $N_8^2$  calculated every 0.04 MPa.



## 8 $\epsilon$

We cannot yet tell whether any dissipation rates measured in the mixed layer are distinguishable from the ship's wake. The Brown and other ships with Z-drives have deeper propellers than most of the other ships we have worked on. At our request, the ship ran at constant rpm to avoid the propeller bursts that occur when the auto-pilot makes course corrections.

Although very intermittent, dissipation rates show the same wedge deepening below the mixed layer that are shown in the other variables( Fig. 13). There are also at least three intermittent upward lines matching the near-inertial phase lines.

Changing the colormap reveals  $\epsilon$  events expanding vertically beneath the mixed layer in the same pattern first seen with  $\theta$  (Fig. 3). In more detail, the dissipation seems to lie along parallel bands rising in depth with time and seem to be associated with bands of alternating high and low stratification seen in the lower panel of Figure 10. A primary goal of analysis should be determining whether these in fact lie along the phase lines of downward propagating near-inertial motions. There is also a sustained burst of turbulence in the deep section where  $\mathbf{Fr}^2$  is elevated. Although similar, the two patterns are far from identical. In particular, why didn't we observe more mixing during the end of the deep  $\mathbf{Fr}^2$  maximum?

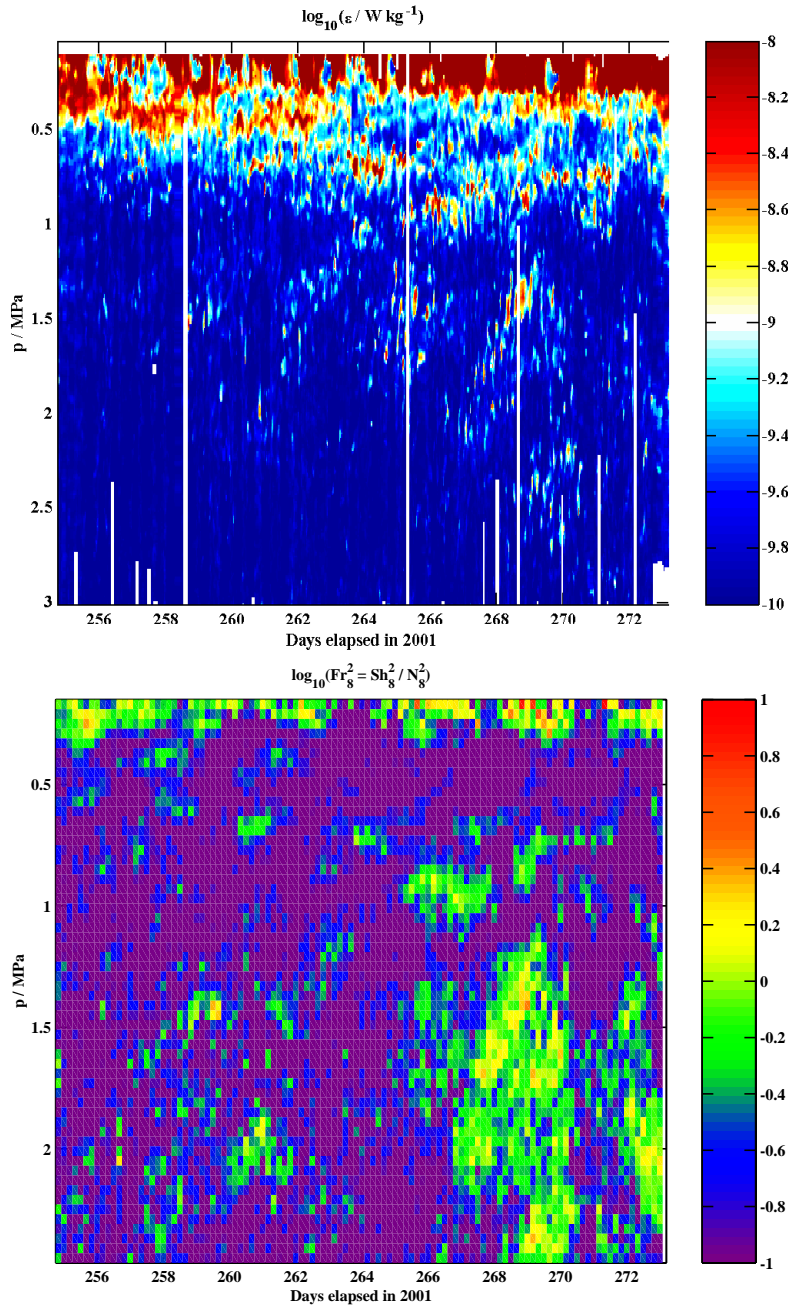


Figure 13:  $\log_{10} \epsilon$  compared with  $\log_{10} Fr^2$ .

## 9 Diapycnal Diffusivity

The diapycnal diffusivity is computed from microstructure measurements as  $K_\rho = 0.2\epsilon N^{-2}$ . As before, the  $\epsilon$  array was median filtered before  $K_\rho$  was calculated. Levels in Figure 14 are very low in the thermocline, negligible in fact, but deeper show the near-inertial phase lines.

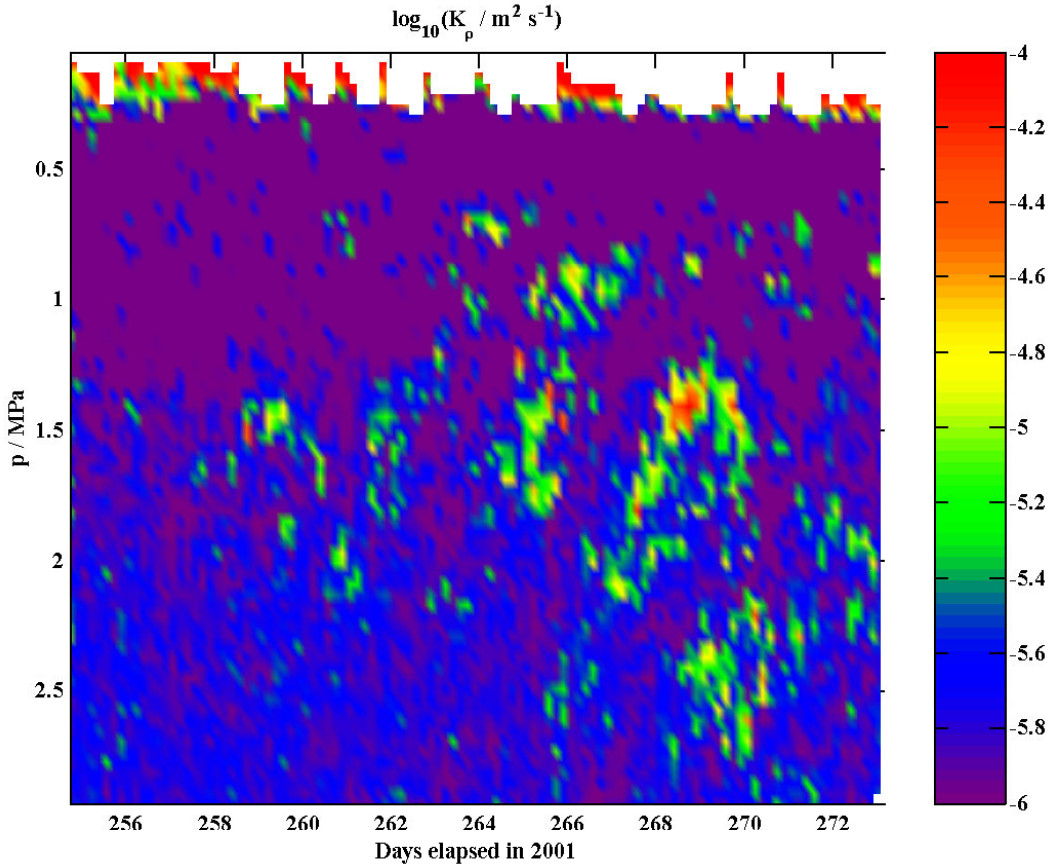


Figure 14:  $\log_{10}(K_\rho/\text{m}^2 \text{ s}^{-1})$  with data averaged over 0.04 MPa and 4 hours. Interpolated shading. Values shallower than the calculated mixed layer depth have been set to nans and are white on the plot.

Because dissipation in the mixed layer has been removed, the large diffusivities at the top of the plot are presumably the ones mixing the surface layer with the thermocline. This is shown in more detail in Figure reffig.ShallowFluxes which repeats the shallow potential temperature and compares it with  $K_\rho$  and  $J_B = K_\rho N^2 = 0.2\epsilon$ . These show a wide range of diapycnal diffusivities and associated buoyancy fluxes at the base of the mixed layer.

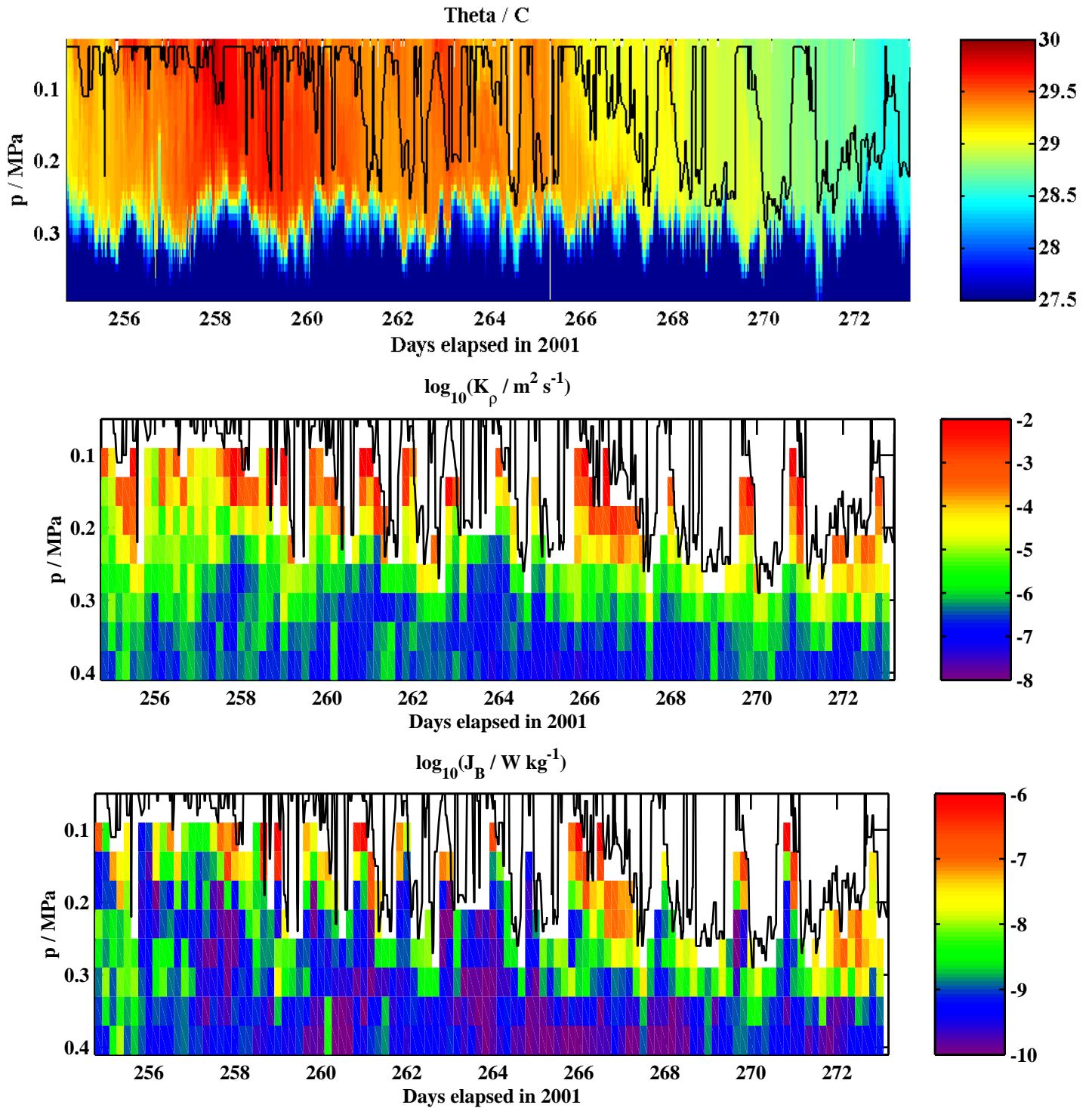


Figure 15: From top to bottom: shallow  $\theta$ ,  $K_\rho$ , and  $J_B$ . Same data intervals as previous figure. Mixed layer depth is overlaid.